

## PIN LNR40339 - BRONZE - BRONZE AGE - SWITZERLAND

<b>Artefact name</b>	Pin Lnr40339
<b>Authors</b>	Brechbühl, Sabine (archaeological service canton Bern, Bern, Bern, Switzerland) & Naima, Gutknecht (HE-Arc CR, Neuchâtel, Neuchâtel, Switzerland) & Valentina, Valbi (Laboratoire Métallurgie et Culture LMC-IRAMAT-CNRS-UTBM, Belfort, Franche-Comté, France)
<b>Url</b>	/artefacts/1255/

### ∨ The object

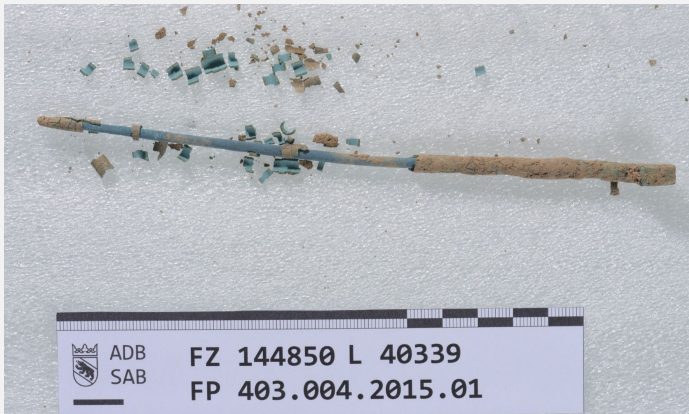


Fig. 1: Pin with surface flaking,

*Credit Archaeological Service Canton Bern.*

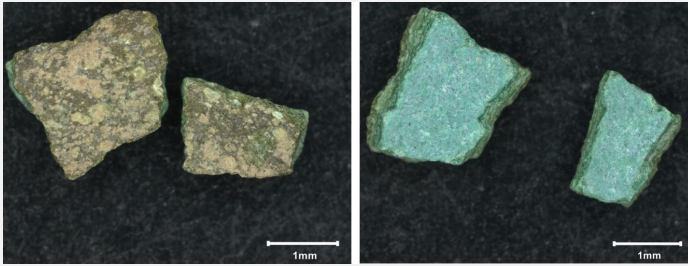
### ∨ Description and visual observation

<b>Description of the artefact</b>	Pin with a curved head. The corroded surface is light brown and there is internal blue corrosion visible where the upper layers flaked. Dimensions: L = ca. 12cm. D = ca. 0.5cm.
<b>Type of artefact</b>	Jewellery
<b>Origin</b>	Kehrsatz, Breitenacker, Kehrsatz, Bern, Switzerland
<b>Recovering date</b>	2015
<b>Chronology category</b>	Bronze Age
<b>chronology tpq</b>	<input type="text"/> ---- ▾
<b>chronology taq</b>	<input type="text"/> ---- ▾
<b>Chronology comment</b>	Found in disturbed layers of soil during excavation, therefore no chronology can be clearly deduced.
<b>Burial conditions / environment</b>	Soil
<b>Artefact location</b>	archaeological service canton Bern, Bern, Bern
<b>Owner</b>	archaeological service canton Bern, Bern, Bern
<b>Inv. number</b>	Lnr. 40339
<b>Recorded conservation data</b>	The object was cleaned of soil with ethanol. The flaking of corrosion was glued back and consolidated with Paraloid B-72.

### Complementary information

None.

Study area(s)



Credit LMC-CNRS, V.Valbi.

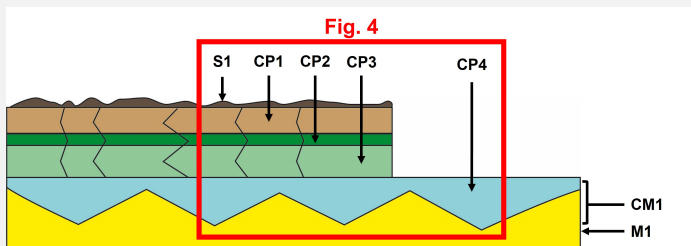
Fig. 2: Fragments of the entire corrosion structure detached from the object and collected before restoration for the study. Appearance of the external (left) and internal (right) surfaces of the fragments,

Binocular observation and representation of the corrosion structure

The schematic representation below gives an overview of the corrosion structure encountered on the pin from a first visual macroscopic observation.

Strata	Type of stratum	Principal characteristics
S1	Soil	brown, thin, limons microstructure, discontinuous, non compact, very soft
CP1	Corrosion product	light brown, medium, discontinuous, compact, soft
CP2	Corrosion product	dark green, thin, discontinuous, compact, soft
CP3	Corrosion product	light green, medium, discontinuous, compact, soft
CP4	Corrosion product	pale turquoise, medium, continuous, non compact, very soft
CM1	Corroded metal	Layer, average ratio (50/50) between CP4 and M1
M1	Metal	yellow, metallic, compact, soft

Table 1: Description of the principal characteristics of the strata as observed under binocular and described according to Bertholon's method.



Credit HE-Arc CR, N.Gutknecht.

Fig. 3: Stratigraphic representation of the corrosion structure of the pin by macroscopic and binocular observation with location of Fig. 4,

MiCorr stratigraphy(ies) – Bi

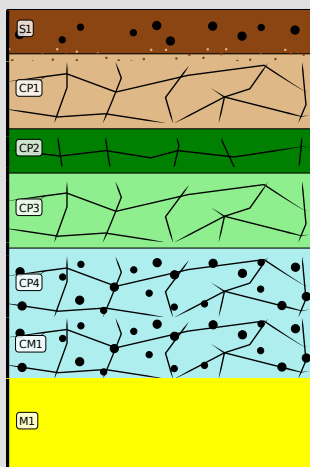


Fig. 4: Stratigraphic representation of the corrosion structure of the pin observed macroscopically under binocular microscope using the MiCorr application with reference to Fig. 3. The characteristics of the strata are only accessible by clicking on the drawing that redirects you to the search tool by stratigraphy representation, Credit HE-Arc CR, N.Gutknecht.

Sample(s)

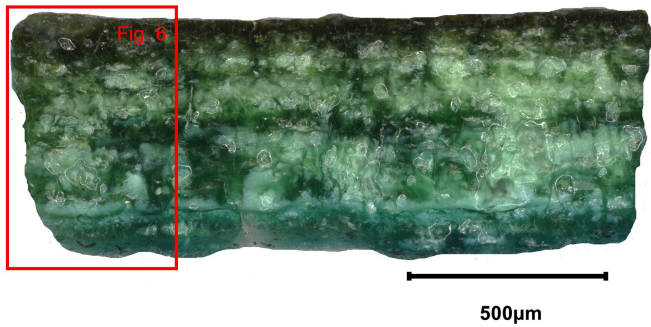


Fig. 5: Micrograph of the cross-section of the fragment from the pin (Fig. 2, left fragment) in dark field showing the location of Fig. 6. The external surface is on top,

Credit LMC-CNRS, V.Valbi.

<b>Description of sample</b>	The sample is a fragment (a flake) of the corrosion stratigraphy that spontaneously detached from the object (Fig. 5).
<b>Alloy</b>	Bronze
<b>Technology</b>	None
<b>Lab number of sample</b>	
<b>Sample location</b>	archaeological service canton Bern, Bern, Bern
<b>Responsible institution</b>	archaeological service canton Bern, Bern, Bern
<b>Date and aim of sampling</b>	May 2021

**Complementary information**

None.

∨ **Analyses and results**

*Analyses performed*

**Invasive approach (on the sample)**

- Optical microscopy: the sample is polished, then it is observed with a numerical microscope KEYENCE VHX-7000 in bright and dark field.
- SEM-EDX: the sample is coated with a carbon layer and analyses are performed on a SEM-FEG JEOL 7001-F equipped with a silicon-drift EDX Oxford detector (Aztec analysis software) with an accelerating voltage of 20 kV and probe current at about 9 nA. The relative error is considered of about 10% for content range <1mass%, and of 2% for content range of >1mass%.
- $\mu$ -Raman spectroscopy: it is performed on a HORIBA Labram Xplora spectrometer equipped with a 532 nm laser with 1800 grating, the laser power employed is between 0.04 and 0.55 mW with acquisition time varying between 1 and 5 minutes.

∨ **Non invasive analysis**

None.

∨ **Metal**

From the observation of the colour of the pin in the central part where the corrosion stratigraphy got detached, we can assume that the metal is a copper-based alloy. The analysis of the corrosion stratigraphy (see next section) indicates that it might be a bronze.

<b>Microstructure</b>	None
<b>First metal element</b>	Cu
<b>Other metal elements</b>	

## Complementary information

None.

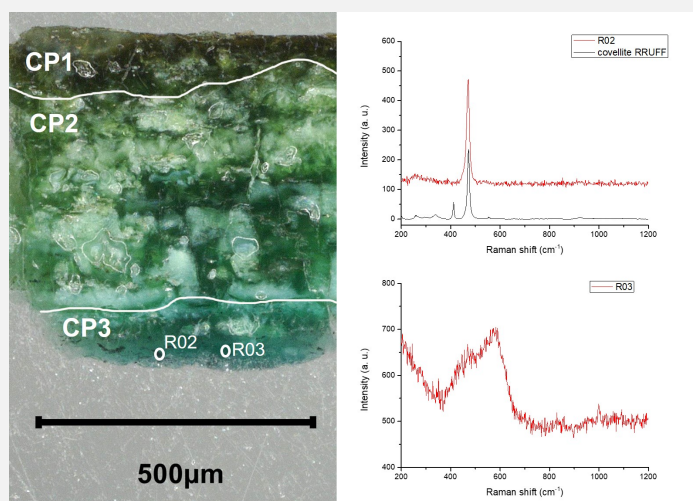
### Corrosion layers

The observation of the sample in cross-section in dark field (Fig. 6) allowed to identify an external 150  $\mu\text{m}$  thick brown stratum (CP1), a green 400  $\mu\text{m}$  thick stratum (CP2), and a blue 150  $\mu\text{m}$  thick stratum (CP3). The EDX analysis (Table 2) shows that the whole corrosion structure has a low Cu content and a much higher Sn content, suggesting then that the metal is a bronze where the corrosion stratigraphy is Cu depleted (14 mass%) and Sn enriched (51 mass%) with none or low polluting elements from external source (Si, P, Al, Fe, Ca, Cl). Dark inclusions mainly observable in the CP3 layer were also analysed and are believed to be copper sulphide. They might be residual metal inclusions.

$\mu$ -Raman analyses were performed on the three identified strata but it was not possible to obtain a clear signal for CP1 and CP2 strata. For the blue CP3 stratum the spectrum obtained has a broad peak at 560  $\text{cm}^{-1}$  that can be attributed to nanocrystals of cassiterite  $\text{Sn}_2\text{O}$  thanks to comparison with the work of Ospitali et al. 2012. The  $\mu$ -Raman analysis performed on the dark inclusions showed a spectrum with a peak at 470  $\text{cm}^{-1}$  compatible with that of covellite ( $\text{CuS}$ ).

	CP1	CP2	CP3	CP3 - inclusion
O	30	31	31	3
Sn	51	51	50	10
Cu	14	14	14	57
S	< 0.5	< 0.5	< 0.5	< 0.5
Si	2	1	1	< 0.5
P	1	1	1	n.d.
Al	1	< 0.5	< 0.5	n.d.
Pb	1	1	1	n.d.
Cl	< 0.5	< 0.5	< 0.5	n.d.

Table 2: Chemical composition (mass%) of the corrosion layers over a general area of analysis in cross-section obtained by SEM-EDX, LMC-IRAMAT-CNRS-UTBM.



Credit LMC-CNRS, V.Valbi.

Fig. 6: Micrograph of the corrosion stratigraphy with the subdivision of the different strata from Fig. 5 (detail), dark field with location of Raman analysis points and the respective obtained spectra of covellite for R02 (RRUFFID=R060306) and nanocassiterite for R03 as determined by comparison of the work of Ospitalie et al. 2012,

Corrosion form Uniform

Corrosion type None

## Complementary information

None.

### MiCorr stratigraphy(ies) – CS

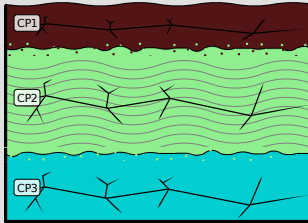


Fig. 7: Stratigraphic representation of the sample of pin observed in cross-section under dark field using the MiCorr application. The characteristics of the strata are only accessible by clicking on the drawing that redirects you to the search tool by stratigraphy representation. This representation was build according to Fig. 6, Credit LMC-CNRS, V.Valbi.

#### ✎ Synthesis of the binocular / cross-section examination of the corrosion structure

One sediment stratum and 4 CPs were identified by binocular observation on the whole object, while only 3 CPs were identified by cross-sectional observation on one flake of the corrosion stratigraphy. The binocular description allows to discriminate more strata based on texture parameters that do not correspond to clear differences observable in cross-section, thus more than one stratum observed by binocular corresponds to only one stratum in cross-section. The outer sediment layer (S1) and the CP1 identified by the binocular observation coincide with the CP1 observed in cross-section, while the CP2 and CP3 observed by binocular coincide with the CP2 in cross-section. The blue CP4 in binocular coincide with the blue CP3 in cross-section.

The metal is not represented in cross-section as the analysis was carried out on a fragment of the corrosion stratigraphy that spontaneously got detached from the object. In this case, the double approach by binocular and cross-section observation is particularly useful and allows to have a more comprehensive understanding of the object with minimal sampling.

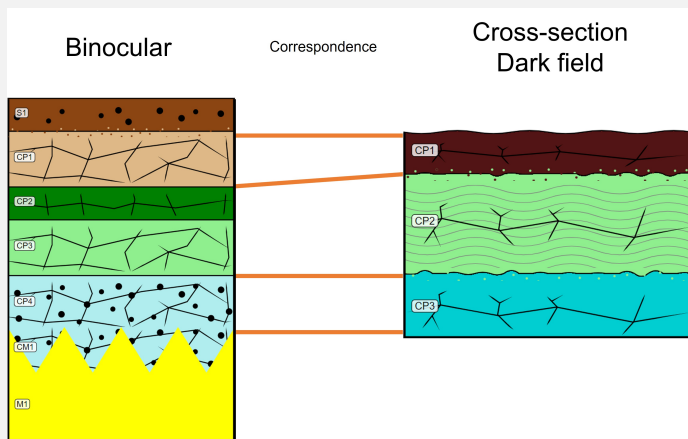


Fig. 8: Stratigraphic representation side by side of binocular view and cross-section (dark field),

#### ✎ Conclusion

Although the metal has not been analysed, the EDS analysis of the corrosion stratigraphy (low Cu content and high Sn content) seems to indicate that the pin is made of bronze with a typical decuprification phenomenon. The dark covellite compounds in CP3 (cross-sections) are most likely residual of copper sulfide inclusions from the metal microstructure.

There is no available documentation to establish if the flaking of corrosion appeared before or after drying the object. Some analyses were performed on corrosion samples before treatment and didn't lead to a conclusive result to explain the flaking phenomenon (Dietze-Uldry, 2020). The current study is done on an untreated flake of the corrosion structure put aside before treatment. Other objects with flaking corrosion were studied, some common features were found (presence of copper sulfide, presence of hydroxycarbonates, high porosity and cracking of the CPs...) but cannot explain completely the flaking phenomenon and more investigation is needed.

#### ✎ References

##### References on analytical methods and interpretation

1. Lafuente, B., Downs, R. T., Yang, H., Stone, N. (2015) The power of databases: the RRUFF project. In: Highlights in Mineralogical Crystallography, T. Armbruster and R. M. Danisi, eds. Berlin, Germany, W. De Gruyter, 1-30.
2. Ospitali, F., Chiavari, C., Martini, C., Bernardi, E., Passarini, F., Robbiola, L. (2012) The characterization of Sn-based corrosion products in ancient bronzes: a Raman approach. *Journal of Raman Spectroscopy*, 43 (11), 1596-1603.
3. Robbiola L., Blengino M., Fiaud C., (1998) Morphology and mechanisms of formation of natural patinas on archaeological Cu-Sn alloys. *Corrosion Science*, 40 (12), 2083-2111.
4. Dietze-Uldry, S. Prétôt. L. Kehrsatz, Breitenacher – Un type de corrosion inconnu sur une épingle de l'Age du Bronze. *Archéologie bernoise*, 2020. P. 52-54.

